

## Synthesis and Characterization of Hematite Nanoparticles as Active Photocatalyst for Water Splitting Application

CHIN Sze Mei<sup>1,A</sup>, SURIATI Sufian<sup>1,B</sup> And Jeefferie Abdul Razak<sup>2,C</sup>

<sup>1</sup>Chemical Engineering Department, Universiti Teknologi PETRONAS, Bandar Seri Iskandar 31750, Tronoh, Perak, Malaysia

<sup>2</sup>Engineering Materials Department, Faculty of Manufacturing Engineering Universiti Teknikal Malaysia Melaka, Hang Tuah Jaya, 76100, Durian Tunggal, Melaka, Malaysia

<sup>a</sup>grace90csm@gmail.com, <sup>b</sup>suriati@petronas.com.my, <sup>c</sup>jeefferie@utem.edu.my

**Keywords:** hematite; self-combustion; photo catalyst; water splitting; hydrogen production

**Abstract.** This paper highlights on the hydrogen production through photocatalytic activity by using hematite nanoparticles synthesized from self-combustion method based on different stirring period. The morphologies and microstructures of the nanostructures were determined using Field-Emission Scanning Electron Microscope (FESEM), X-Ray Diffractometer (XRD) and Particle Size Analyser (PSA). Besides that, surface area analyser was used to determine the BET surface area of the hematite samples. The hematite nanocatalyst as-synthesized are proven to be rhombohedral crystalline hematite ( $\alpha$ -Fe<sub>2</sub>O<sub>3</sub>) with particle diameters ranging from 60-140 nm. The BET specific surface area of hematite samples increased from 5.437 to 7.6425 m<sup>2</sup>/g with increasing stirring period from 1 to 4 weeks. This caused the amount of hydrogen gas produced from photocatalytic water splitting to increase as well.

### Introduction

Renewable energy and environmental issues are highly emphasized globally in order to reduce and replace the use of fossil fuels in various sectors. Thus, the research on hydrogen gas production has been done since decades ago as an alternative fuel for renewable energy. Photocatalytic water splitting to produce hydrogen gas has been studied in the research fields of catalysis, electrochemistry, photochemistry, organic and inorganic chemistry since the discovery of Honda-Fujishima effect by using a TiO<sub>2</sub> semiconductor electrode in hydrogen production [1]. Water splitting is an uphill reaction which utilizes sunlight to break down water into hydrogen and oxygen. It is also known as an artificial photosynthesis. The photon energy from the sunlight is converted to chemical energy with a large positive change in Gibbs energy ( $G_0 = +237.2$  kJ/mol) [2]. Since TiO<sub>2</sub> photocatalyst can only make use of the UV radiation which occupies only 4% of the solar energy [3], many photocatalysts with better properties have been developed in order to replace TiO<sub>2</sub>.

From all of the photocatalysts discovered and developed, hematite ( $\alpha$ -Fe<sub>2</sub>O<sub>3</sub>) has been synthesized to be one of the candidates developed for photocatalysis in water splitting application. It is in the form of iron (III) oxide and is considered as the most stable iron oxide. It has emerged as one of the promising photocatalysts in water splitting application because of its attractive properties such as small band gap (2.1 eV), high resistivity to corrosion, low cost and abundant [4]. It is also widely used in magnetism, lithium ion battery and gas sensors [5]. Hematite nanostructures can be in the form of zero-dimensional (0-D) such as nanoparticles and one-dimensional (1-D) which includes nanowires, nanorods, nanobelts and nanotubes.

Up to date, there are various methods being used to synthesize hematite nanostructures, namely thermal oxidation of iron [5,6,7], hydrothermal synthesis [8], improved synthetic strategy [5], surfactant assisted synthesis [9], template-free hydrothermal method [10] and also sol-gel method [11]. However, synthesis of hematite nanostructures using self-combustion method is still limited and under investigation. In addition, the effects of stirring period on the characteristics of the hematite nanostructures produced from self-combustion method have yet to be known from the studies. Thus,

the aim of the research is to synthesize and characterize hematite nanostructures using self-combustion method based on different stirring period and observe their effects on photocatalytic activity to produce hydrogen gas from water.

## Methodology

**Synthesis of Hematite Nanocatalyst.** The hematite nanocatalyst was synthesized by using self-combustion method. Initially, 66.82 g of iron (III) nitrate,  $\text{Fe}(\text{NO}_3)_3 \cdot 9\text{H}_2\text{O}$  was dissolved in 334.1 mL of 65% nitric acid,  $\text{HNO}_3$ . The mixture was stirred vigorously on a hot plate at  $28^\circ\text{C}$  by using a magnetic stirrer for 1 week to obtain a homogeneous solution. The homogeneous solution was heated gradually until it combusted at temperature of  $110^\circ\text{C}$ . The gelatine was dried in an oven at  $110^\circ\text{C}$  for overnight. The dried sample was crushed by using mortar and pestle and annealed at  $700^\circ\text{C}$  in a furnace for three hours to get hematite nanocatalyst. The steps were repeated by changing the stirring period of the mixture to 2, 3 and 4 weeks respectively. The samples were labeled as S1, S2, S3 and S4 with respect to the stirring period time of 1, 2, 3 and 4 weeks.

**Characterization of Hematite Nanocatalyst.** The hematite nanocatalyst samples obtained were sent for characterization by using X-Ray Diffractometer (XRD), Particle Size Analyser (PSA), Field-Emission Scanning Electron Microscope (FESEM) and Brunauer-Emmett-Teller (BET) surface area analyser. The XRD patterns of the samples were taken using a Bruker-AXS D8 Advance diffractometer with  $\text{Cu-K}\alpha$  radiation ( $= 1.5406 \text{ \AA}$ ) operating at 60 kV and 80 mA. A scan range of  $20^\circ$ – $80^\circ$  ( $2\theta$ ) was used. The particle size distribution of the hematite nanocatalyst samples were analysed by using PSA by Malvern Instruments. FESEM was used to depict the surface morphology of the samples. This was carried out using Variable Pressure Field-Emission Scanning Electron Microscope (VPFESEM, Zeiss Supra55 VP). BET surface area analyser was used to determine the surface area of the samples. The model used was Micromeritics ASAP 2020 via nitrogen adsorption. The sample preparation was divided into 2 stages where the first stage was performed at  $90^\circ\text{C}$  for 30 minutes at ramping rate of  $10^\circ\text{C}/\text{min}$ . The second stage was achieved at  $200^\circ\text{C}$  for 240 minutes at the same ramping rate of  $10^\circ\text{C}/\text{min}$ .

**Measurement of Photocatalytic Activity.** The performance of the hematite as-synthesized was determined through photocatalytic activity by quantifying the amount of hydrogen produced. One gram of S1 hematite nanocatalyst sample was mixed in 100 mL of distilled water in a conical flask with side arm. A magnetic stirrer was placed inside the mixture solution and the conical flask tightly was covered using a stopper. The side arm was connected with a small tube and it was immersed into another small conical flask with water. The conical flask containing the mixture solution was placed on top of a hot plate with stirrer. A visible light lamp was installed beside the conical flask. The visible light and the hot plate were switched on. The stirring rate and temperature were set at 300 rpm and  $50^\circ\text{C}$  respectively. The experimental setup was covered by a box to in order to maximize the light produced by the lamp. The amount of bubbles released from the small tube immersed in small conical flask was recorded for 15 minutes. After 15 minutes of experiment, the light and hot plate were switched off. The amount of hydrogen produced from the solution was detected. The procedure was repeated with S2, S3 and S4 hematite nanocatalyst samples.

## Results and discussion

**Synthesis of Hematite Nanocatalyst.** Four of the hematite nanocatalyst samples synthesized have been sent for XRD to study the crystallography of the samples. Fig. 1 below shows the XRD patterns of the hematite nanocatalyst samples after stirring for (a) 1 week, (b) 2 weeks, (c) 3 weeks and (d) 4 weeks, respectively. The peaks shown in the figure matched with the standard hematite sample (JCPDS Card No. 33-0664,  $a = b = 5.0353 \text{ \AA}$  and  $c = 13.7495 \text{ \AA}$ ) [5,9,10,12]. The samples showed strong peaks at [012], [104], [110], [024], [116], [214] and [300] which prove that the hematite samples obtained are rhombohedral crystalline hematite ( $\alpha\text{-Fe}_2\text{O}_3$ ). The major XRD peaks for all the

samples were obtained at  $2\theta=33.15^\circ$  while the second major peaks were observed at  $2\theta=35.7^\circ$ . The diameters of the samples are determined by using Scherrer equation. The diameter of sample S1 is found to be 470.91 nm and the diameter increases to 471 nm for sample S4. It can be seen that the particle size increased from S1 to S4 with increasing stirring period.

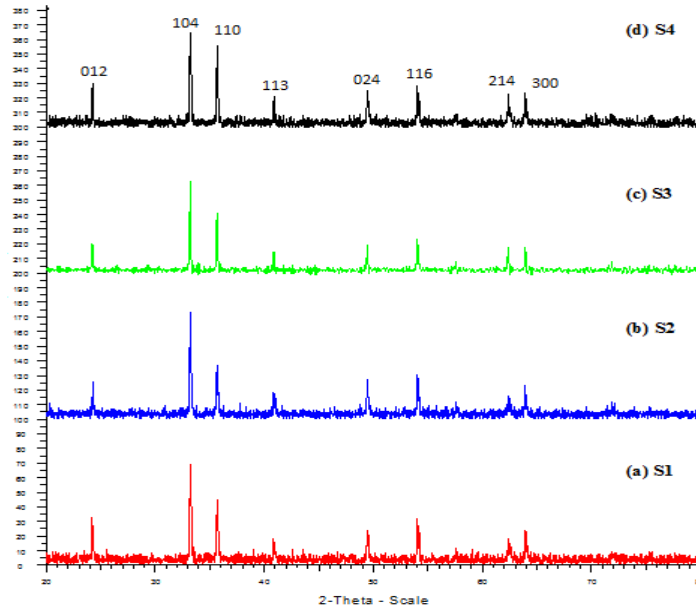


Fig. 1. XRD patterns of the hematite nanocatalyst after stirring for (a) 1 week, (b) 2 weeks, (c) 3 weeks and (d) 4 weeks respectively.

The particle size distribution of the hematite nanocatalyst samples are shown in Fig. 2. From the particle size distribution graphs of the samples, it can be seen that most of the particles in samples S1, S2 and S3 are distributed in the size of  $4.7 \mu\text{m}$  and  $170 \mu\text{m}$  while most of the particles in sample S4 are distributed in the size of  $0.59 \mu\text{m}$  and  $5.5 \mu\text{m}$ . The particle sizes of the hematite nanocatalyst samples determined by PSA are larger than the particle sizes obtained from XRD. This is because PSA can only detect the size of the particles that agglomerate together into larger particles, which results in larger particles size distribution of the hematite nanocatalyst samples.

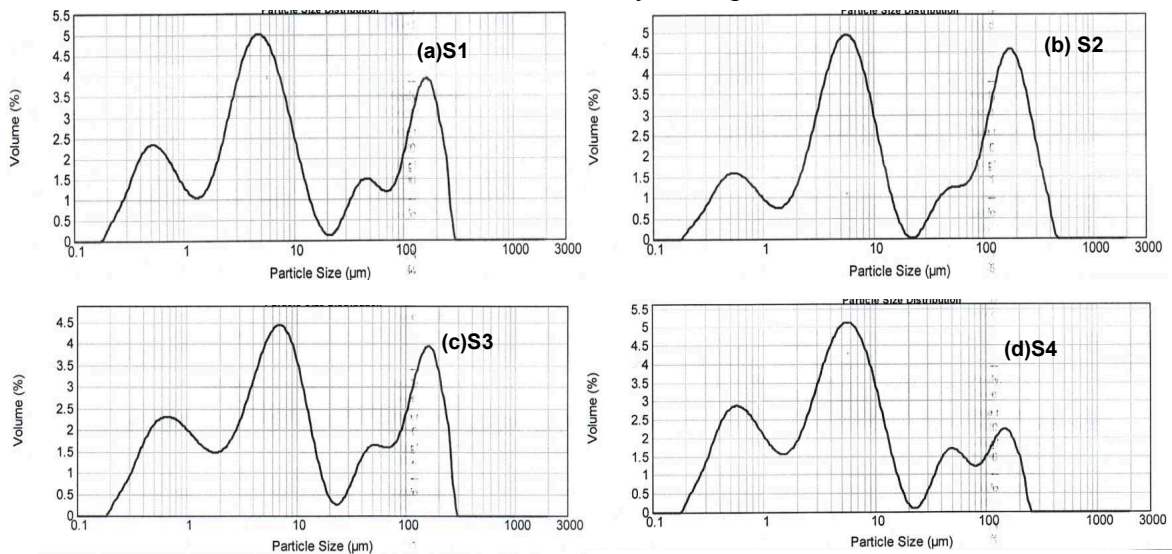


Fig. 2. Particle size distribution for sample (a) S1, (b) S2, (c) S3 and (d) S4.

Fig. 3(a) shows the FESEM image of S1 hematite nanocatalyst sample that has been stirred for 1 week. From the image, it is clearly shown that the hematite nanocatalyst appeared in spherical shape. The diameters of the as-grown hematite nanocatalyst are distributed in the range of 60–120 nm. The EDX spectrum of S1 hematite nanocatalyst sample can be referred to Fig. 4(a). The sample exhibits

the presence of Fe, O and a small amount of C in weight percentage of 52.03%, 37.83% and 10.13% respectively. This has proven that the as-synthesized sample is  $\alpha$ -Fe<sub>2</sub>O<sub>3</sub>. On the other hand, Fig. 3(b) shows the FESEM image of S4 hematite nanocatalyst sample which has been stirred for 4 weeks. The hematite nanocatalyst occurred in spherical shape as well. The diameters of the hematite nanocatalyst are distributed in the range of 90–140 nm, which are slightly larger than S1 hematite nanocatalyst. The EDX spectrum of S4 hematite nanocatalyst sample in Fig. 4(b) shows that Fe, O and C are present in 59.70%, 34.42% and 5.88% respectively. Thus, the sample is proven to be  $\alpha$ -Fe<sub>2</sub>O<sub>3</sub>.

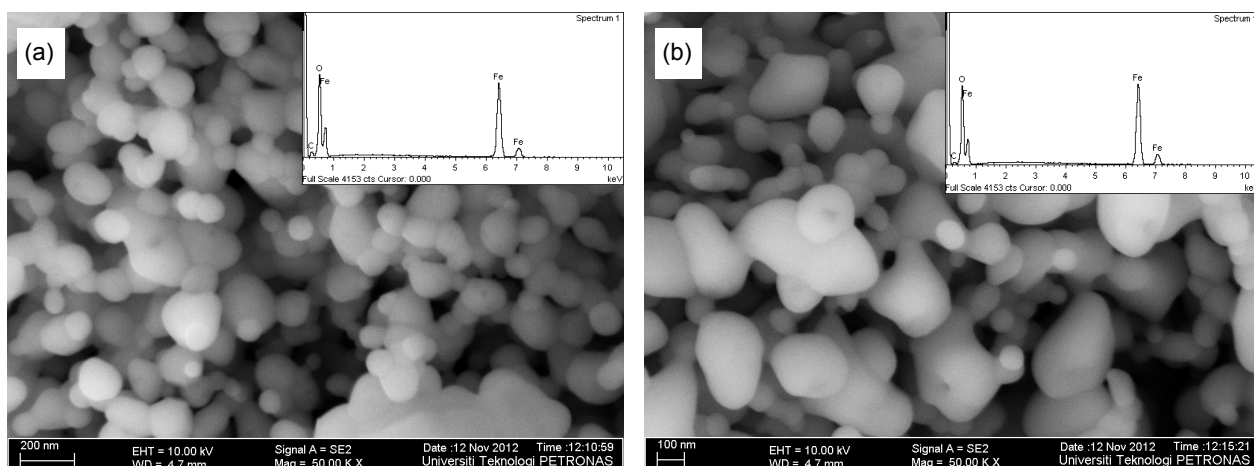


Fig. 3. FESEM images of (a) S1 and (b) S4 hematite nanocatalyst. Insets showed the EDX spectrum for each of the samples.

The surface area of S1, S2, S3 and S4 hematite nanocatalyst samples were determined by using Brunauer-Emmett-Teller surface area analyser (BET). The BET surface area, pore volume and pore size of each of the hematite nanocatalyst sample are shown in Table 1. From the results obtained, it is shown that S4 hematite nanocatalyst sample has the highest surface area, which is 7.6425 m<sup>2</sup>/g while sample S1 has the lowest surface area, which is 5.4537 m<sup>2</sup>/g. From here, it is obvious that the BET surface area increases as the stirring period increases. As the stirring period is increased, the mixture of iron (III) nitrate and nitric acid will have more time to react with each other and the particles can disperse themselves evenly throughout the solution. This will prevent the particles from agglomerate together and thus giving higher surface area.

Table 1. BET specific surface area and amount of hydrogen produced of S1, S2, S3 and S4 hematite nanocatalyst samples.

Sample	BET specific surface area (m <sup>2</sup> /g)	Amount of H <sub>2</sub> produced × 10 <sup>-7</sup> (g/s)
S1	5.437	6.59
S2	5.9316	4.09
S3	6.0831	4.35
S4	7.6425	4.75

Based on the research works done by Juncosa (2008), it is found that the BET surface area of hematite is 14.92 m<sup>2</sup>/g [13]. Besides that, Wu et. al. (2006) stated that the BET surface areas of the hematite nanostructures synthesized using improved synthetic strategy range from 5.9 to 52.3 m<sup>2</sup>/g [8]. From here, it can be seen that the BET surface areas of the four hematite nanocatalyst samples are slightly lower than that from the studies. This might be due to the agglomeration of the particles which caused the nitrogen hard to be adsorbed into the particles during the BET analysis, thus leading to lower surface area of the samples.

**Measurement of Photocatalytic activity.** For the measurement of photocatalytic activity, all four samples are being tested in order to determine which sample can produce more hydrogen gas from water. From the experiment, it is found that S4 sample produced highest amount of hydrogen gas among the four samples. For 1g of S4 in 100 mL of distilled water, 4.75 × 10<sup>-6</sup> g/s of hydrogen gas is being produced during 15 minutes of the experiment. The summary of the amount of hydrogen gas produced is shown in the Table 1. The amount of hydrogen gas produced from the hematite

nancatalyst samples can be explained from the BET surface areas of the samples. The higher the BET surface area of the samples, the higher the amount of hydrogen gas produced from the samples. This is because the higher surface area of hematite results in more active sites on the particles. With more active sites available, the reactions to produce hydrogen gas from the water molecules using the equations as shown below can take place effectively.

### Conclusion

In summary, the hematite nanocatalyst samples synthesized using self-combustion method are proven to be rhombohedral crystalline hematite ( $\alpha$ -Fe<sub>2</sub>O<sub>3</sub>) from XRD results. The hematite nanocatalyst showed spherical in shape as depicted in the FESEM images obtained. The diameters of the hematite samples were ranging from 60–140 nm which showed that they were in nano size. The BET surface area of the four samples increased with increasing stirring period. This affects the photocatalytic performance of the hematite samples in producing hydrogen gas from water. The amount of hydrogen gas produced increased with increasing surface area of the samples due to more active sites available on the particles.

### Acknowledgements

The authors would like to thank Universiti Teknologi PETRONAS for providing the facilities and support during the accomplishment of the research work.

### References

- [1] A. Fujishima, T.N. Rao, and D.A. Tryk, *Titanium dioxide photocatalysis*, Journal of Photochemistry and Photobiology, 1-21. (2000).
- [2] A. Kudo, and Y. Miseki, *Heterogeneous photocatalyst materials for water splitting*. Chemical Society Review, 253-278. (2009).
- [3] X. Lian, X. Yang, S. Liu, Y., Xu, C. Jiang, J. Chen, et al. *Enhanced photoelectrochemical performance of Ti-doped hematite thin films prepared by the sol-gel method*. Applied Surface Science 258, 2307-2311. (2010).
- [4] R. Wang, Y. Chen, Y. Fu, H. Zhang, H and C. Kisielowski, *Bicrystalline Hematite Nanowires*. J. Phys. Chem. B, 12245-12249. (2005).
- [5] C. Wu, P. Yin, C. OuYang, and Y. Xie, *Synthesis of Hematite ( $\alpha$ -Fe<sub>2</sub>O<sub>3</sub>) Nanorods: Diameter-Size and Shape Effects on Their*. J.Phys. Chem. B, 17806-17812. (2006)
- [6] P. Hiralal, S. Saremi-Yarahmadi, B.C. Bayer, H. Wang, S. Hofmann, K.U. Wijayantha, K. U., et al. *Nanostructured hematite photoelectrochemical electrodes prepared by the low temperature thermal oxidation of iron*. Solar Energy Materials & Solar Cells, 1819-1825. (2011).
- [7] T. Vincent, M. Gross, H. Dotan, and A. Rothschild, *Thermally oxidized iron oxide nanoarchitectures for hydrogen production by solar-induced water splitting*. International Journal of Hydrogen Energy, 8102-8109. (2012).
- [8] G.L. Chiarello, L. Forni I. Rossetti, and E. Selli, *Photocatalytic water splitting on different oxide-based systems*. <http://users.unimi.it/upg/articoli/turku2.pdf>
- [9] L. Liu, H. Z. Kou, W. Mo, H. Liu, and Y. Wang, Y. *Surfactant-Assisted Synthesis of  $\alpha$ -Fe<sub>2</sub>O<sub>3</sub> Nanotubes and Nanorods with Shape-Dependent*. J. Phys. Chem. B, 15218-15223. (2006).
- [10] S. Zeng, K. Tang, and T. Li, T. *Controlled synthesis of  $\alpha$ -Fe<sub>2</sub>O<sub>3</sub> nanorods and its size-dependent optical*. Journal of Colloid and Interface Science, 513-521. (2007).
- [11] J.G. Kim, K.H. Han, C.H. Lee, and J.Y. Jeong, *Crystallographic and Magnetic Properties of Nanostructured Hematite Synthesized by the Sol-Gel Process*. Journal of the Korean Physical Society, 798-802. (2001)
- [12] C. Liu, J. Ma, and Y. Liu, *Formation mechanism and magnetic properties of three different hematite nanostructures synthesized by one-step hydrothermal procedure*. SCIENCE CHINA, 1607-1614. (2011).
- [13] E.C. Juncosa, *Adsorption Properties of Synthetic Iron Oxides: As (V) Adsorption on Geothite ( $\alpha$ -FeOOH)*. D Master Thesis, 2-31. (2008).